ELSEVIER

Journal of Alloys and Compounds 375 (2004) 292–296

Journal of ALLOYS AND COMPOUNDS

www.elsevier.com/locate/jallcom

Effect of the nature of the starting materials on the formation of Mg_2FeH_6

F.J. Castro [a,b,*], F.C. Gennari [c]

[a] *Comisión Nacional de Energía Atómica (CNEA), Centro Atómico Bariloche, R8402AGP-S.C. de Bariloche, Argentina*
[b] *Instituto Balseiro (UNC and CNEA), Centro Atómico Bariloche, R8402AGP-S.C. de Bariloche, Argentina*
[c] *Consejo Nacional de Investigaciones Científicas y Técnicas, CONICET, Centro Atómico Bariloche, R8402AGP-S.C. de Bariloche, Argentina*

Received 9 September 2002; received in revised form 1 September 2003; accepted 28 November 2003

Abstract

The compound Mg_2FeH_6 was synthesized in a single process by reactive mechanical alloying (RMA) a $2MgH_2 + Fe$ mixture under hydrogen atmosphere at room temperature. The process yield is 15.6 wt.% of Mg_2FeH_6, after 100 h of milling. The synthesis of Mg_2FeH_6 takes almost twice the time and gives nearly half the yield obtained when milling a $2Mg + Fe$ mixture under similar conditions. The differences observed are explained in terms of the contrast between the mechanical properties and the microstructures of the starting mixtures.

Keywords: Hydrogen storage material; Mechanical alloying; Thermal analysis

1. Introduction

Magnesium has been thoroughly studied as a hydride forming material due to several advantages, such as its high hydrogen capacity by weight (7.6 wt.%, theoretical value), its abundance in the earth's crust, and its low cost. However, its main drawbacks are its high stability and low hydrogen absorption–desorption kinetics. In this perspective, the family of compounds Mg_2NiH_4, Mg_2CoH_5 and Mg_2FeH_6 appears as an interesting alternative, compromising hydrogen capacity for better hydriding and dehydriding kinetics. In this family, the compound Mg_2FeH_6 has the peculiarity that the intermetallic Mg_2Fe has not been observed in a stable form. As a consequence of this, the synthesis of the hydride becomes a rather difficult task. Previously Mg_2FeH_6 has been obtained by sintering Mg and Fe powders at high H_2 pressures (∼100 bar) and temperatures of the order of 500 °C for several days [1,2]. An improvement in the synthesis of Mg_2FeH_6 was made when mechanical alloying (MA) was used to obtain the hydride [3–7].

There are four main alternatives to obtain Mg_2FeH_6 using MA: (a) milling Mg and Fe in an inert atmosphere (e.g. Ar) and then hydriding the material, (b) milling Mg and Fe under a H_2 atmosphere (reactive mechanical alloying, RMA), (c) milling MgH_2 and Fe in an inert atmosphere, and (d) milling MgH_2 and Fe under H_2 atmosphere. Huot et al. [5,6] have explored alternatives (a), (b) and (c). When milling Mg and Fe elemental powders, independently of the atmosphere used, they have found that the milling products have to be submitted to a sintering process after milling (∼24 h at 350 °C under 0.5 MPa of H_2) in order to obtain Mg_2FeH_6. When milling MgH_2 with Fe in an inert atmosphere they were able to synthesize Mg_2FeH_6 as a milling byproduct. We have previously followed alternative (b) [7] to synthesize Mg_2FeH_6 using a low energy milling device, and surprisingly found that we did not need to sinterize the milling products to obtain Mg_2FeH_6. We also found there that the most probable reaction path to Mg_2FeH_6 was MgH_2 formation followed by reaction of this hydride with Fe to produce Mg_2FeH_6.

In this work we present the synthesis of Mg_2FeH_6 by following alternative (d). In principle, the advantage of this synthesis route would be that by providing MgH_2 from the start of the milling, the first step in the reaction path to Mg_2FeH_6 could be skipped. This could lead to a reduction on the synthesis time and/or an increment in the product yield.

* Corresponding author. Fax: +54-2944-445299.
E-mail address: fcastro@cab.cnea.gov.ar (F.J. Castro).

0925-8388/$ – see front matter © 2003 Elsevier B.V. All rights reserved.
doi:10.1016/j.jallcom.2003.11.147

2. Experimental

Magnesium hydride (MgH_2) powder (90%) and iron granules (>99%) were mechanically milled under hydrogen atmosphere, using a Uni-Ball-Mill II apparatus (Australian Scientific Instrument). The $2MgH_2 + Fe$ mixture (mixture A), together with ferromagnetic steel balls were placed in a stainless steel container and enclosed in an argon glove box. The container was then evacuated to 10^{-5} MPa prior to filling with 0.5 MPa of electrolytic hydrogen (99.99999%). The samples were milled for different times up to a total of 140 h and the container was systematically refilled with hydrogen every 5 h in order to keep the hydrogen pressure constant. The ball to powder weight ratio was 44:1.

At regular intervals, the container was opened in an argon dry box and a small amount of powder was taken for analysis by X-ray powder diffraction (XRD), scanning electron microscopy (SEM), and differential scanning calorimetry (DSC). The X-ray powder diffraction was performed on a Philips PW 1710/01 Instruments with Cu Kα radiation (graphite monochromator). Scanning electron microscopy (SEM 515, Philips Electronic Instruments) was used to characterize the microstructure of the powders by using mounted and polished samples. The thermal behavior of the compound was studied by DSC (DSC 2910, TA Instruments) with a 6 °C min^{-1} heating rate and an argon flow rate of 18 ml min^{-1}.

3. Results and discussion

In Fig. 1 the evolution of the powder mixture with milling time (mt) can be followed by means of several XRD patterns. After 10 h mt the initial phases (tetragonal β-MgH_2, JCPDS Powder Diffraction Data Card No. 12–0697) and Fe (JCPDS Powder Diffraction Data Card No. 06–0696) are observed, together with a small reflection corresponding to orthorhombic γ-MgH_2 (JCPDS Powder Diffraction Data Card No. 35–1184) [8] and two small peaks associated to MgO (JCPDS Powder Diffraction Data Card No. 45–0946). From 20 to 60 h mt, the evolution is characterized by a gradual reduction of the intensity and a widening of the MgH_2 peaks (Fe reflections do not change significantly in this period). After 80 h mt, a couple of peaks corresponding to Mg_2FeH_6 (JCPDS Powder Diffraction Data Card No. 38–0843) can be seen (weakly present at 60 h mt). Also, at this milling time, the reflections of Fe slightly appear with a small reduction in their intensity, and the peaks associated with MgH_2 disappear, probably due to the formation of Mg_2FeH_6, the intense amorphization and the simultaneous reduction of crystallite size induced by milling. At 100 h mt the reflections of Mg_2FeH_6 attain its maximum value. Further milling only produces a decrease in the intensity of Mg_2FeH_6 reflections, and an increase in the MgO peaks.

Fig. 2 shows the DSC curves of the samples milled up to 100 h. The curve corresponding to 10 h mt (Fig. 2A) presents an endotherm located around 370 °C associated with the decomposition of MgH_2. This decomposition temperature is substantially lower than that of non-milled MgH_2 ~450 °C. The reduction in this temperature is a consequence of both the microstructural changes induced by milling and a catalytic effect produced by Fe [4,7]. After 40 h mt, the

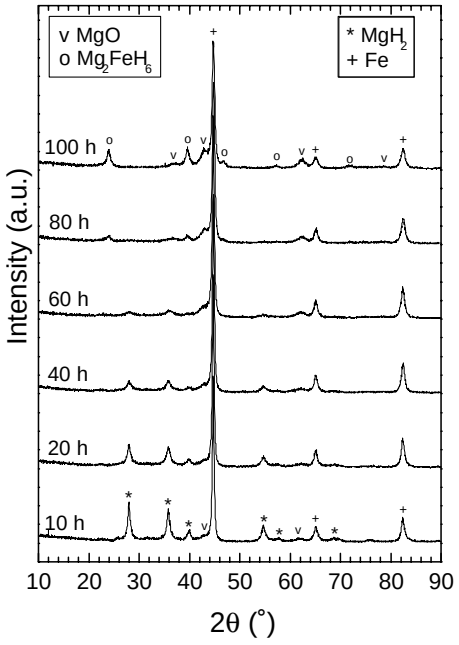

Fig. 1. X-ray diffraction patterns of the $2MgH_2 + Fe$ mixture after RMA, as a function of milling time.

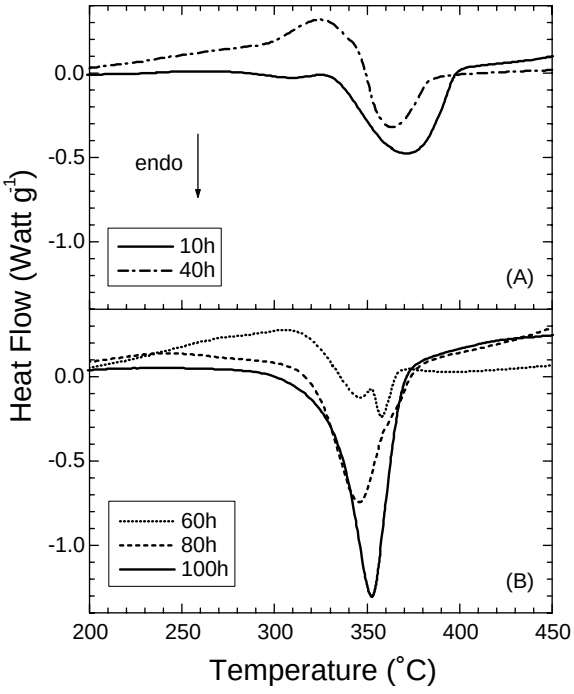

Fig. 2. DSC curves of mixture A after RMA as a function of milling time: (A) 10 and 40 h, and (B) 60, 80 and 100 h.

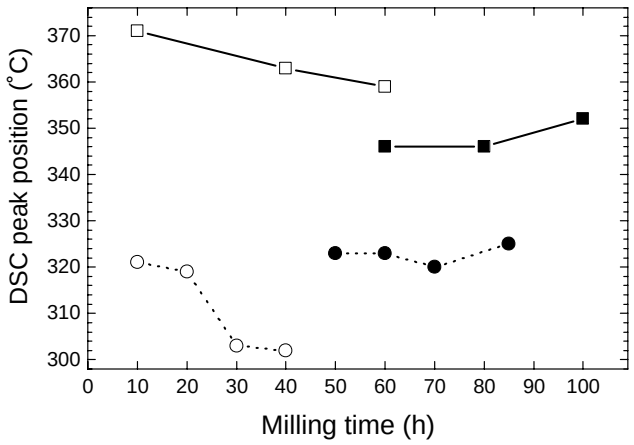

Fig. 3. DSC peak position (temperature of the minimum of the endotherms) for MgH_2 decomposition (open symbols) and Mg_2FeH_6 decomposition (solid symbols) for mixture A (MgH_2 + Fe, squares) and mixture B (2Mg + Fe, circles), as a function of milling time.

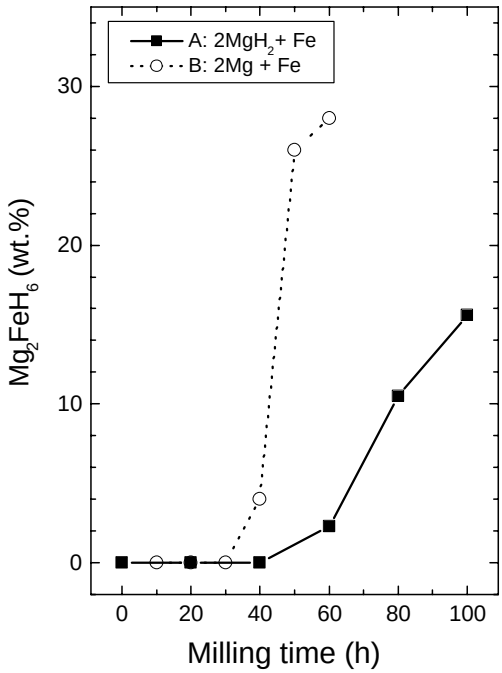

Fig. 4. Amount of Mg_2FeH_6 as determined from DSC curves for mixture A (MgH_2 + Fe, squares) and mixture B (2Mg + Fe, circles), as a function of milling time.

endotherm shifts a few degrees towards lower temperatures, mostly as a consequence of reduction of particle size and better intermixing of MgH_2 and Fe particles. When the mixture is milled 60 h, the DSC curves show an endotherm composed of two peaks, the small one (lower temperature) can be linked to Mg_2FeH_6 decomposition and the other one to MgH_2 decomposition. After 80 h mt (Fig. 2B), the double peak observed at 60 h resolves in a deeper endotherm associated with Mg_2FeH_6 decomposition. After 100 h mt the endothermic peak of Mg_2FeH_6 decomposition with the greatest area is observed. By further milling, the area of the peaks decreases, in accordance with XRD information.

The evolution of the temperature of the peaks is compared in Fig. 3 with the behavior observed when milling a 2Mg + Fe mixture (mixture B) under similar conditions [7]. For shorter milling (less than 60 h for mixture A and 40 h for mixture B), the endotherms correspond to MgH_2 decomposition, and their position shift towards lower temperatures with increasing mt. Also, we observe that the decomposition temperatures in the case of mixture B are ∼50 °C lower than the decomposition temperatures for mixture A. As will be discussed below, this behavior shows a more efficient intermixing of the materials of mixture B, which can be linked with microstructural and mechanical differences between both mixtures. For longer milling times, the endotherms are associated with Mg_2FeH_6 decomposition. In this case, the position of the peaks does not change significantly with milling time (indeed, it presents a small shift towards higher temperatures), but the decomposition temperatures in the case of mixture B are still lower than the corresponding ones of mixture A. In this case, the gap reduces to ∼25 °C.

By using the reported value of the enthalpy of formation of Mg_2FeH_6, 98 kJ mol^{-1} H_2, an estimation of the amount of hydride can be made. Up to 40 h mt no Mg_2FeH_6 was detected. The deconvolution of the curve of 60 h mt gives as a result an amount of Mg_2FeH_6 equal to 2.3 wt.%. At 80 and 100 h mt, the amounts of Mg_2FeH_6 increase to 10.5 wt.% (80 h) and 15.6 wt.% (100 h). After this milling time, the quantity of Mg_2FeH_6 progressively reduces. Consequently, the maximum yield of Mg_2FeH_6 obtained by milling mixture A is 15.6 wt.%, after 100 h of milling. In Fig. 4 we compare the amount of Mg_2FeH_6 as a function of milling time for mixtures A and B. It can be seen that the maximum yield for mixture A is nearly half the maximum yield obtained for mixture B, and it takes almost twice the synthesis time. This result is very surprising, because MgH_2 seems to act as an intermediate product in the reaction path to Mg_2FeH_6 [5,7]. We expected that starting from a $2MgH_2$ + Fe mixture would result in a higher yield and a lower synthesis time. We believe that an explanation for this behavior can be found in the morphology, the microstructure and the mechanical properties of the materials milled.

Fig. 5 shows SEM images obtained with backscattered electrons of the mixture B (Fig. 5A) and of the mixture A (Fig. 5B) after 10 h mt. The brighter phase corresponds to Fe, the other phase is Mg and/or MgH_2. There are clear differences between both mixtures. The mixture B, composed of two ductile substances, produces the typical lamellar structure obtained when a ductile–ductile pair is milled [9]. This microstructure arises as a consequence of the welding of small platelets of Fe and Mg that form during the early stages of milling. During subsequent milling, the lamellae are convoluted, and a very well degree of mixing between the constituents is achieved. On the contrary, mixture A behaves as a ductile–brittle pair, with magnesium hydride playing the role of the brittle material. In this case, the

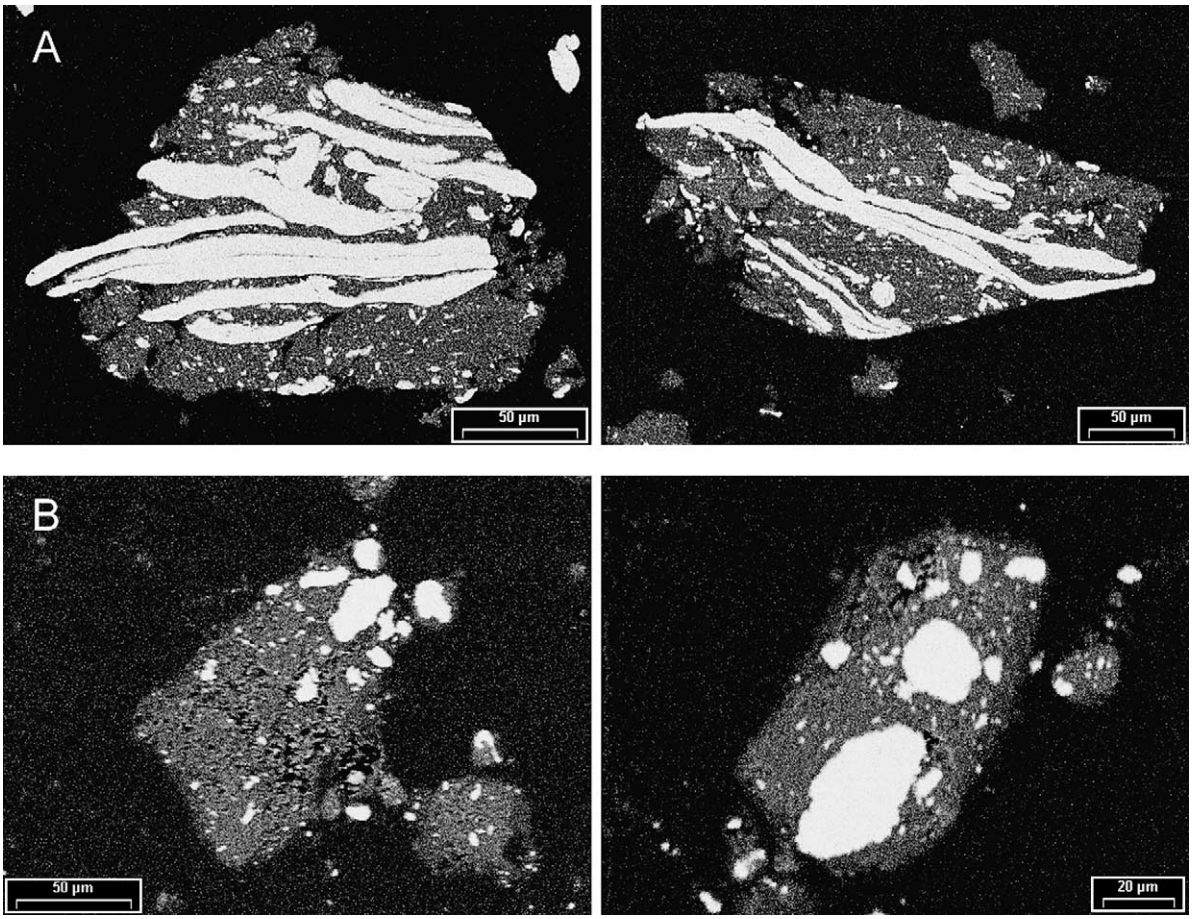

Fig. 5. SEM backscattered electron images after 10 h of RMA of (A) mixture B ($2Mg + Fe$) and (B) mixture A ($2MgH_2 + Fe$).

microstructure is composed of rounded Fe particles surrounded by an agglomerate of MgH_2 powder. The harder MgH_2 particles are not embedded into the Fe particles probably because the volume ratio in the mixture (MgH_2:Fe > 4.5) does not favor such a process. Comparing both microstructures, the lamellar structure of mixture B presents a contact surface between the reactants much greater than the contact area between MgH_2 and the rounded Fe particles observed in mixture A. This traduces in an improved intermixing, which results in higher reactivity, which ends in a small synthesis time and a greater yield in the case of mixture B.

Fig. 6 shows SEM micrographs of both mixtures milled 40 h. Although after this milling time the individual components are better intermixed, Fe particles are still clearly

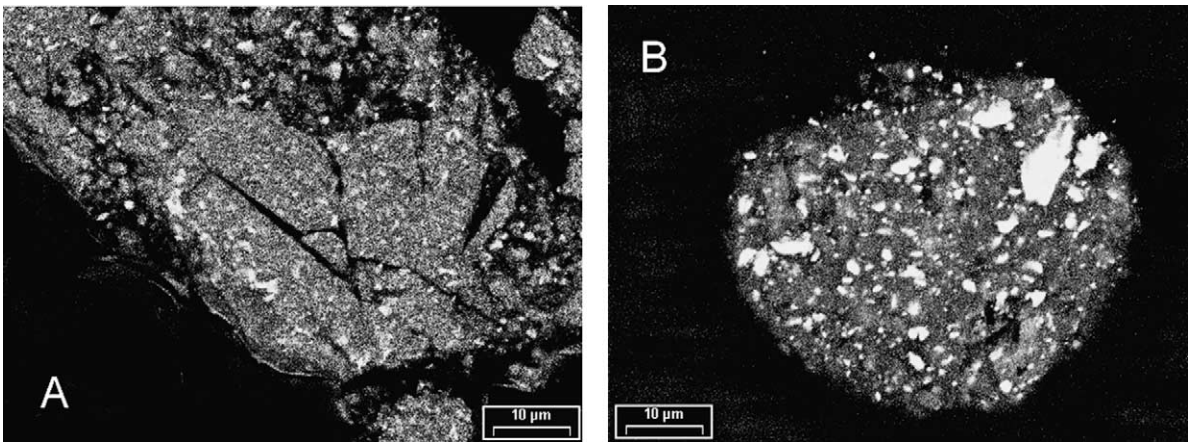

Fig. 6. SEM backscattered electron images after 40 h of RMA of (A) mixture B and (B) mixture A.

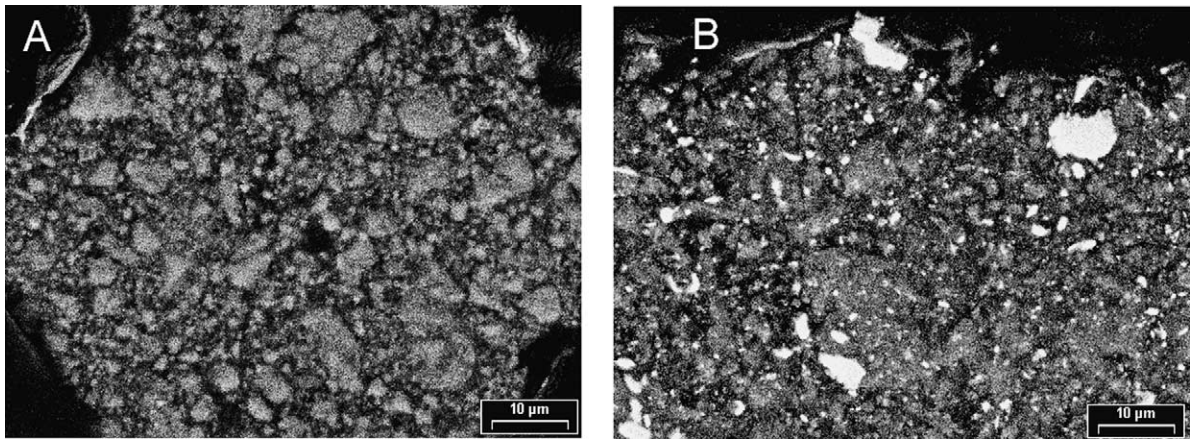

Fig. 7. SEM backscattered electron images of (A) mixture B after 60 h of RMA and (B) mixture A after 100 h of RMA.

visible. In mixture B Fe particle size has reduced to ∼1 μm, while in mixture A particles with sizes up to ∼10 μm can be seen. This difference between the typical sizes of Fe particles (which reflects in a difference in the surface to volume ratio, and hence in the contact area between the reactants) shows that the ductile–ductile combination of Mg and Fe mixture is more efficient in achieving a good intermixing and size reduction. Again, this traduces in higher reactivity, higher yield and reduced synthesis time.

In Fig. 7 we present the morphology of both mixtures at the milling times when the maximum yield occurs (Fig. 7A: mixture B, 60 h and Fig. 7B: mixture A, 100 h). The image of mixture B shows that after 60 h mt the initial Mg and Fe particles have completely intermixed. No Fe particles can be observed at this magnification. On the contrary, and despite milling has proceeded up to 100 h, the microstructure of mixture A shows that the intermixing of the initial materials is not complete at this mt. Fe particles with sizes up to ∼10 μm can still be seen.

4. Conclusions

We presented the synthesis of Mg_2FeH_6 obtained by mechanically alloying a $2MgH_2 + Fe$ mixture in H_2 atmosphere. The product was obtained in one step, without involving any sintering process. The synthesis method elapsed 100 h of milling, and the yield of Mg_2FeH_6 was 15.6 wt.%, as determined from the area of DSC curves. The synthesis time almost doubles, and the yield is nearly half the value obtained when milling a $2Mg + Fe$ mixture in similar experimental conditions (same milling device, equal ball to powder ratio, etc.). We attribute the differences between both synthesis routes mainly to the unlike mechanical properties and microstructures of the mixtures. The $2Mg + Fe$ mixture behaves as a ductile–ductile pair that results in a higher contact surface between Mg and Fe, and a better intermixing and size reduction. These characteristics traduce in a higher yield and a short synthesis time. On the contrary, the $2MgH_2 + Fe$ mixture performs as a ductile–brittle combination, with less contact area between the reactants and hence lower yield and longer synthesis time.

Acknowledgements

The authors thank Fundación Balseiro for partial financial support to carry out this work.

References

[1] J.-J. Didisheim, P. Zolliker, K. Yvon, P. Fisher, J. Schefer, M. Gubelmann, A.F. Williams, Inorg. Chem. 23 (1984) 1953.
[2] P. Selvam, K. Yvon, Int. J. Hydrogen Energy 16 (9) (1991) 615.
[3] E. Ivanov, Y. Konstanchuk, A. Stepanov, V. Boldyrev, J. Less-Common Met. 131 (1987) 25.
[4] Y.G. Konstanchuk, E. Ivanov, M. Pezat, B. Darriet, V. Boldyrev, P. Hagenmuller, J. Less-Common Met. 131 (1987) 181.
[5] J. Huot, H. Hayakawa, E. Akiba, J. Alloys Compd. 248 (1997) 164.
[6] J. Huot, S. Boily, E. Akiba, R. Schulz, J. Alloys Compd. 280 (1998) 306.
[7] F.C. Gennari, F.J. Castro, J.J. Andrade Gamboa, J. Alloys Compd. 339 (2002) 261.
[8] F.C. Gennari, F. Castro, G. Urretavizcaya, J. Alloys Compd. 321 (2001) 46.
[9] C. Suryanarayana, Prog. Mater. Sci. 46 (2001) 1.